Electric Supplementary Information

Rare-Metal-Free High-Performance Water-Activated Paper Battery: A Disposable Energy Source for Wearable Sensing Devices

Kosuke Ishibashi[1], Shimpei Ono[2], Jun Kamei[3], Koju Ito[4], Hiroshi Yabu[1,4,5,*]

[1]Device/System Group, Advanced Institute for Materials Research (WPI-AIMR), Tohoku University, 2-1-1, Katahira, Aoba-Ku, Sendai 980-8577, Japan

[2]Central Research Institute of Electric Power Industry (CRIEPI), 2-6-1 Nagasaka, Yokosuka-shi, Kanagawa 240-0196, Japan

[3]AMPHIBIO, Ltd., Makerversity, West Goods Entrance, Somerset House, Victoria Embankment, London, WC2R 1LA, United Kingdom

[4]AZUL Energy, Inc., 1-9-1, Ichibancho, Aoba-Ku, Sendai 980-0811, Japan

[5]Open Innovation Center of Hydrogen Science for GX, Advanced Institute for Materials Research (WPI-AIMR), Tohoku University, 2-1-1, Katahira, Aoba-Ku, Sendai 980-8577, Japan

Appendix

S1. ORR activities of AZUL electrocatalysts at neutral electrolyte condition

To assess the ORR activity of AZUL catalysts at neutral electrolyte condition, linear sweep voltammetry (LSV) measurements were performed using a rotating ring disc electrode (RRDE). Figure 1(a) shows the LSV curves of GC, MnO_2, and AZUL electrocatalyst measured at 1,600 rpm rotation speed and pH 7.0 with NaCl as an electrolyte, respectively. The obtained starting potentials, half-wave potentials and maximum current values are also shown in Table 1. The activity of the catalysts and the overvoltage of the cathode of the magnesium air battery depend on the ORR onset potential: the onset potentials of the GC, MnO_2 and AZUL catalysts were 4.99 V vs RHE, 6.58 V vs RHE, and 8.12 V vs RHE, respectively, and at neutral the AZUL catalyst achieved higher values than MnO_2, which is commonly used as a cathode catalyst in metal-air battery including hearing aid batteries, and comparable onset potential to Pt/C. This indicates that the AZUL catalyst has a high ORR activity even in the neutral region.

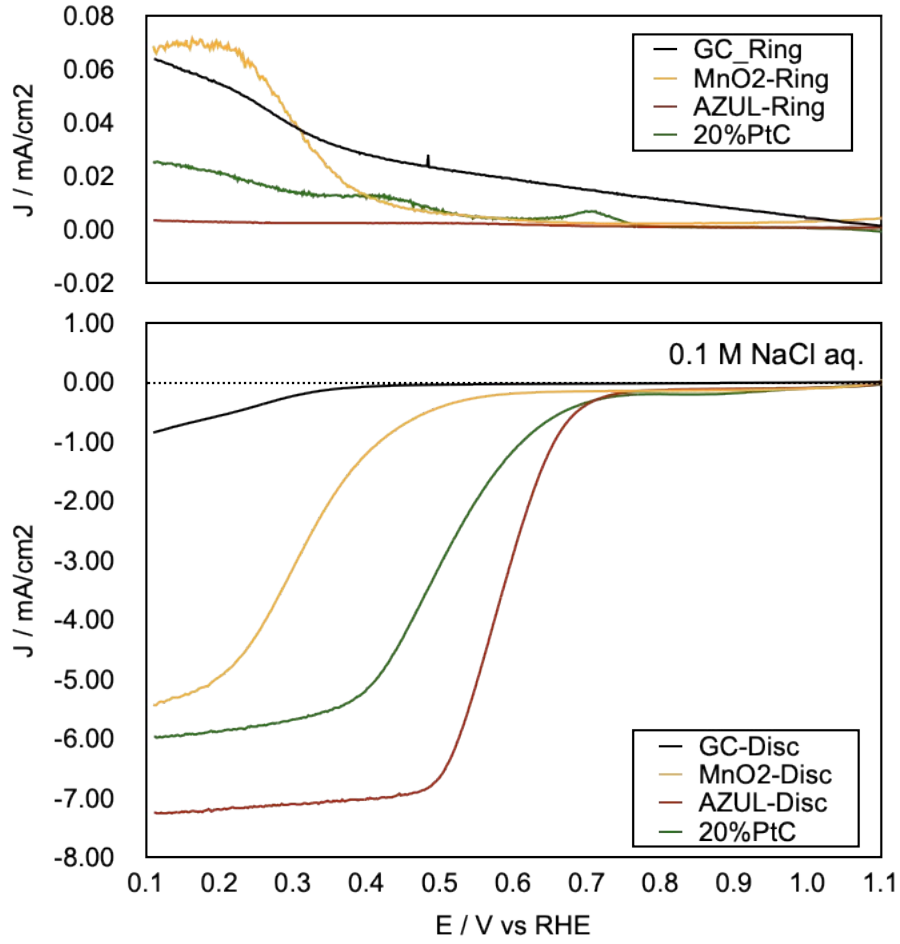

Figure S1. LSV curves on ring and disc electrodes of GC (black), MnO_2 (yellow), Pt/C (green), and AZUL (red) electrocatalysts in 0.1 M NaCl aq., respectively.

The oxygen reduction reaction proceeds in two processes;

$$O_2 + H_2O + 2e^- \rightarrow HO_2^- + OH^- \qquad (1)$$

$O_2 + 2H_2O + 4e^- \rightarrow 4OH^-$ (2)

If the catalyst activity is insufficient, the reaction is a two-electron reaction, (1), giving rise to peroxide ions. On the other hand, the four-electron reaction, (2), proceeds and the oxygen is reduced to hydroxide ions, which is the ideal reaction In RRDE, the amount of hydrogen peroxide produced is estimated by measuring the amount of peroxide ions produced at the disc electrode with immobilized catalyst on a ring disc, and the average reaction in ORR on the catalyst The number of electrons can be calculated from the following equation;

$$n = \frac{4I_D}{I_D + \frac{I_R}{N}} \quad (3)$$

where I_D and I_R are the current densities for the disk and ring electrodes, respectively, and N is the capture efficiency (0.42).

From the hydrogen peroxide generation rate, the number of reaction electrons (n) of ORR on MnO_2 and AZUL electrocatalysts were calculated according to the equation (3). n values of ORR on MnO_2 and AZUL electrocatalysts were 3.85 and 3.99 @0.4 V vs RHE, respectively. The AZUL catalyst showed low hydrogen peroxide generation even in the neutral region of pH 7 and the reaction electron number was close to the ideal value of 4. This shows that the AZUL catalyst exhibits high ORR activity even in the neutral region. Therefore, we used AZUL catalyst as a cathode electrocatalyst.

S2. SEM images of water-absorbing paper sheets

Surface structures of paper sheets were observed by using a scanning electron microscope (SEM, S-5200, Hitach HighTech, Hitachi, Japan). Before observation, Os was sputtered on the surface of spacemen by using a discharge ion sputter (Shinku Kiko, Saitama, Japan). Figure S2 shows SEM images of respective paper sheets. Density of each paper sheet was calculated from weight and volume of the sheet.

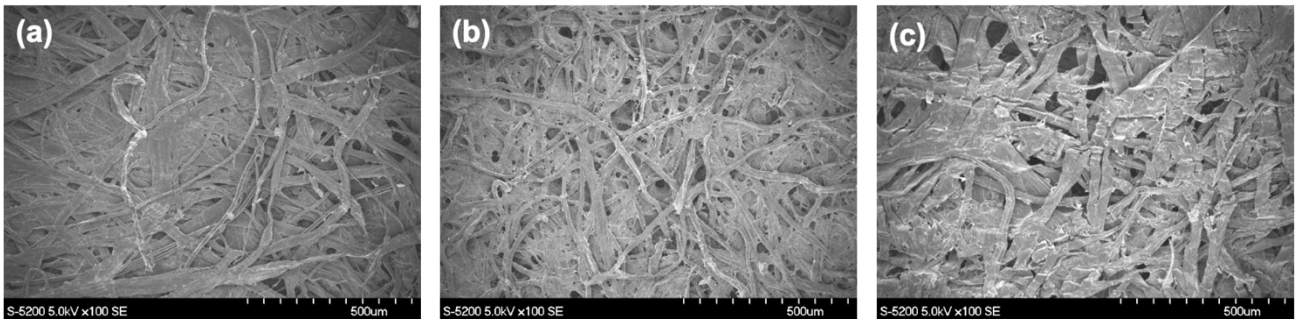

Figure S2. SEM images water-absorbing paper sheets 1 (a), 2 (b), and 3 (c), respectively.

S3. Comparison of Ni mesh and Cu mesh as current correctors

To compare current corrector materials, a Ni-SUS mesh and a Cu mesh were employed to fabricate saltwater-activated paper batteries. Both cells were fabricated according to the experimental section. The water-absorbing paper 2 was used for both cells. I-V polarization curves were measured by potentiostat (Versastat 4) with using 4 M NaCl aq. as an electrolyte.

Figure S3 shows I-V polarization curves of the cells with using Ni-SUS mesh (dotted line) and Cu mesh (solid line). From the plot, the cell with using the Cu mesh was superior performance than that of Ni-SUS mesh.

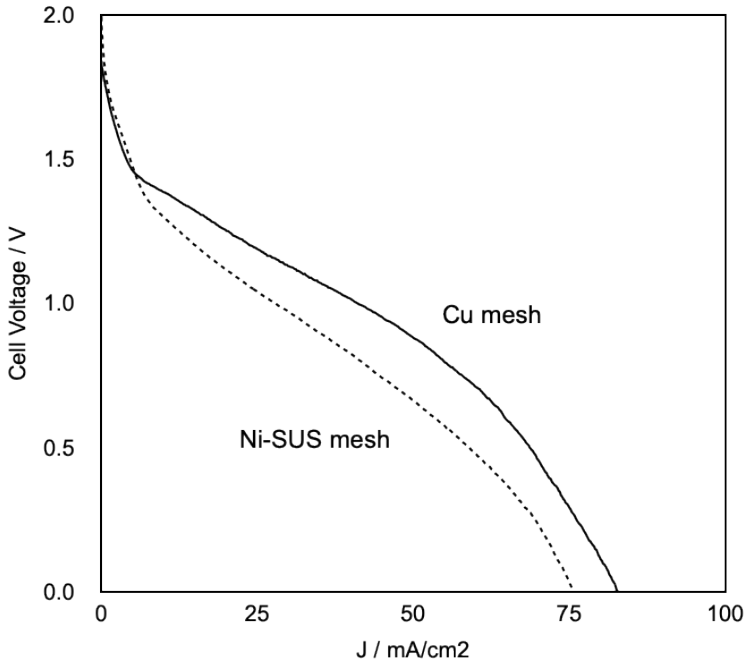

Figure S3. I-V polarization curves of the cells with using Ni-SUS mesh (dotted line) and Cu mesh (solid line).

S4. Specification of a SpO_2 sensor

Figure S4 shows photographs and a circuit diagram of a SpO_2 sensor without cover. On the front side, control IC chip and battery connector were equipped. On the back side, the LED and detector for measuring pulse and O_2 saturation were equipped.

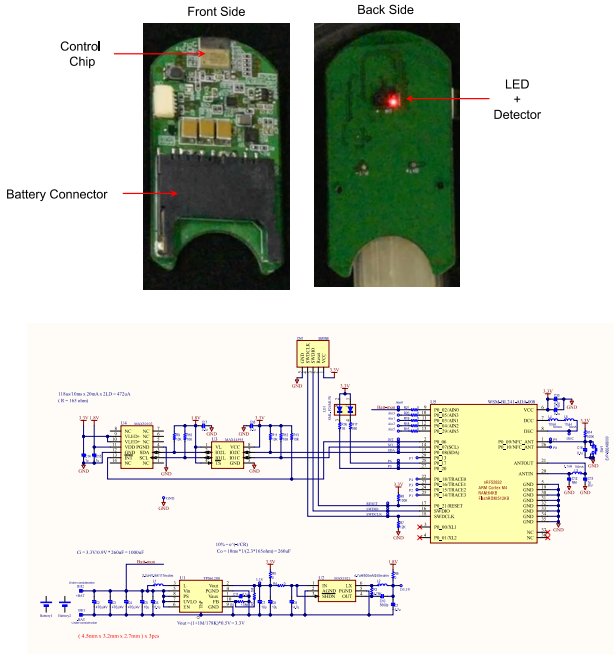

Table S1 shows detail device parameters of the wearable SpO_2 sensor used in this experiment. The device voltage and current were 0.9 V and 5.0 mA, respectively. From those values, required power to drive the device was 4.5 mW. From discharge polarization curves shown in Figure 2(d), the output voltage decreased from c.a. 1.8 V to 0.9 V after 5.45 hours discharging when the discharging current density was 5.0 mA/cm^2. The cathode surface area of the used paper battery cell was fixed as 1.0 cm^2, the device running time equal to the discharging time when the battery voltage reached 0.9 V.

Table S1. Specification of the wearable SpO_2 sensor.

Parameters	Values
Device Voltage [V]	0.9
Device Current [mA]	5.0
Required Power [mW]	4.5
Device Running Time [hours]	5.45

S5. Specification of a GPS logger

Figure S5 shows a photograph of a GPS logger without cover. On the surface side, GPS and other telecommunication antennas and a connector for the paper battery were equipped. On the back side, the LoRa wireless communication IC chip was assembled.

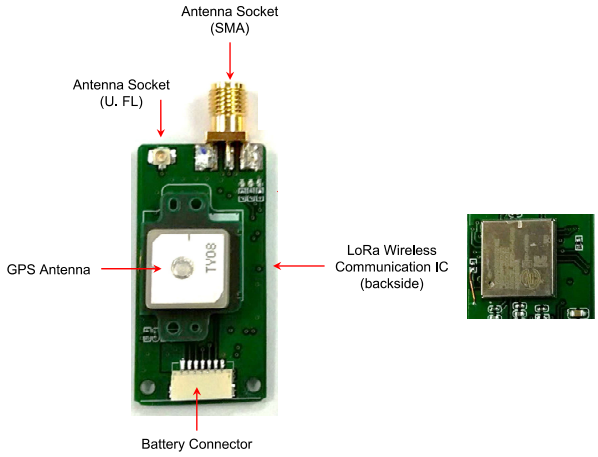

Figure S5. Photograph of GPS logger.

Table S2 shows detail device parameters of the wearable SpO_2 sensor used in this experiment. The device voltage and current were 3.0 V and 3.8 mA, respectively. From those values, required power to drive the device was 11.4 mW.

Table S2. Specification of the wearable GPS logger.

Parameters	Values
Device Voltage [V]	3.0
Device Current [mA]	3.8*
Required Power [mW]	11.4

*Average value of single signal emission with every 120 s.

In order to reduce energy consumption, the device sequence in the GPS logger was optimized. Table S3 shows energy consumption of the device with changing the telecommunication frequency. For life saving, survival rate of the victim of marine disasters significantly decreased after 72 hours (3 days), therefore victim location should be traced at least 3 days. The energy consumption of the device was measured and only 276.3 mAh (=828.9 mWh) used when the telecommunication frequency of one signal/120 s. From this value and the paper battery capacity (968.2 mWh/g), it is enough to use only c.a. 1g Mg foils for paper battery anodes when the 3 serial battery cells are used.

Table S3. Energy consumption with changing the telecommunication frequency.

Telecommunication Frequency [1/sec]	Energy Consumption (1 hour) [mAh]	Energy Consumption (3 days) [mAh]
30	10.2	737.9
60	6.9	497.1
120	3.8	276.3

S6. EIS analysis of cells with current collectors

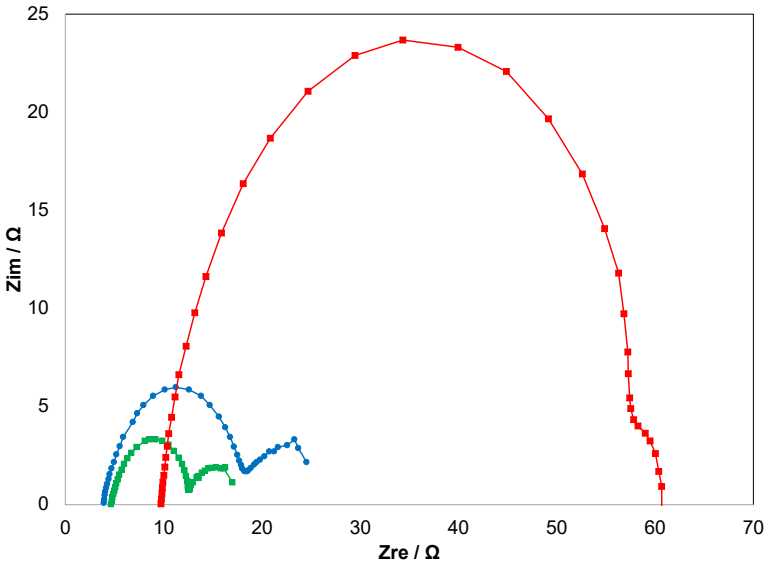

Figure S6. EIS curves of cell 1 (red), cell 2 (green), and cell 3 (blue), respectively.

S7. EIS analysis of cells of a whole disposable cell

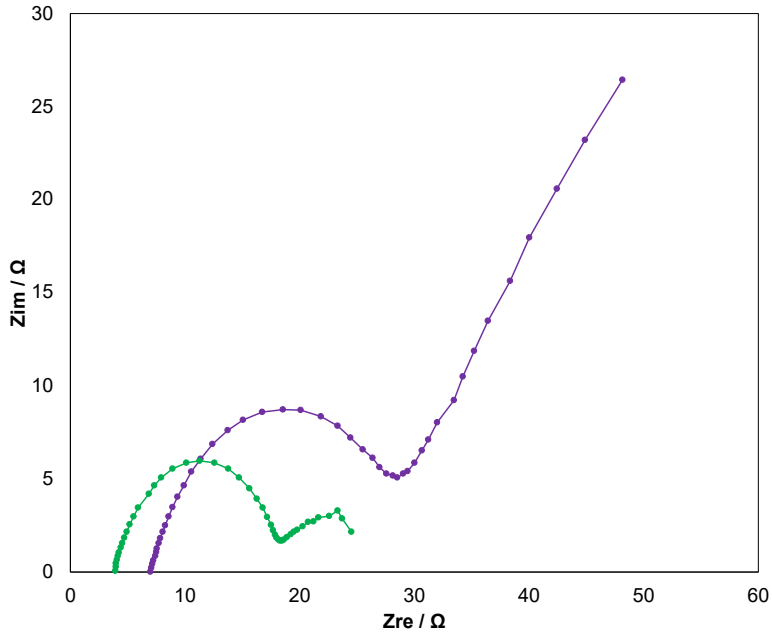

Figure S7. EIS curves of a cell with a Cu current collector (green) and a whole disposable cell (purple), respectively.

S8. Video image of a single battery cell for SpO_2 sensor

See video image, S8.

S9. Video image of 3 serial battery cells for GPS logger

See video image, S9.

S10. Video image of a tree-like disposable battery

See video image, S10.

S11. I-V and I-P polarization curves of optimal paper battery cell

Figure S8 shows I-V and I-P polarization curves of optimal paper battery cell. Those curves obtained by the cell fully uptaken electrolyte after c.a. 20 min. immersion of the paper sheet in the electrolyte. *OCV* and P_{max} of this cell were 1.93 V and 120 mW/cm^2, respectively.

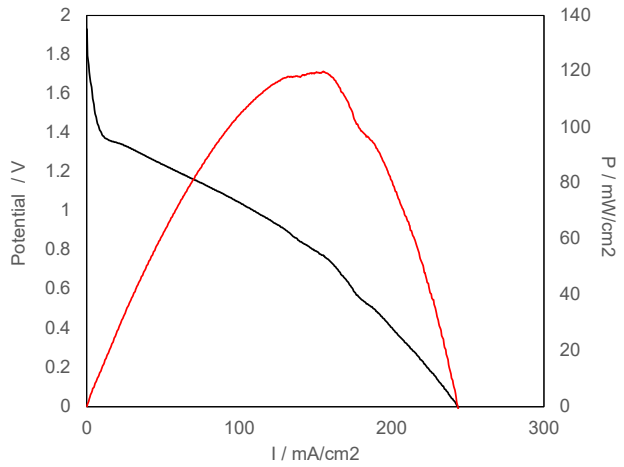

Figure 8. I-V and I-P polarization curves of the optimal paper battery cell.

S12. Video image of SpO_2 sensor activation by current-collector-free paper battery

See video image, S12.

S13. Discharge voltage change under a wet-dry-wet cycle

Figure S9 Shows discharge curves at 5 mA/cm^2 with wet-dry-wet cycles. After one dipping of paper sheet to the electrolyte, the paper battery cell discharged for 2.3 hours and stopped. When electrolyte supplied again, it started discharging again and continued for 2.9 hours. This cycle was confirmed for 3 times. This result indicates that the paper battery discharges for 2-3 hours per one electrolyte supply and the voltage has been recovered by additional supply of the electrolyte.

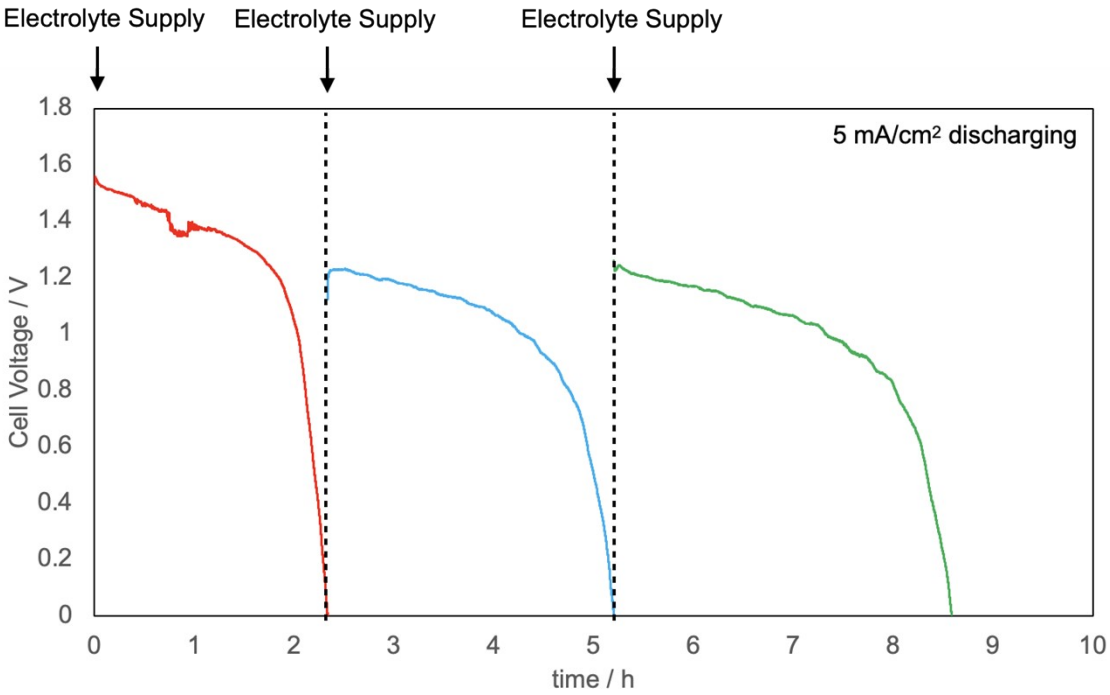

Figure 9. Discharge voltage change under a wet-dry-wet cycle at 5 mA/cm^2 discharging.

S14. Paper battery cell performance with using Pt/C electrocatalyst.

Figure S10 shows I-V and I-P polarization curves of paper battery cell with using Pt/C as a cathode electrocatalyst. *OCV* and P_{max} of this cell were 1.93 V and 109 mW/cm^2, respectively. Those values are almost identical with the cells with using the AZUL electrocatalyst, however, limited current density was much lower than that of AZUL electrocatalyst case.

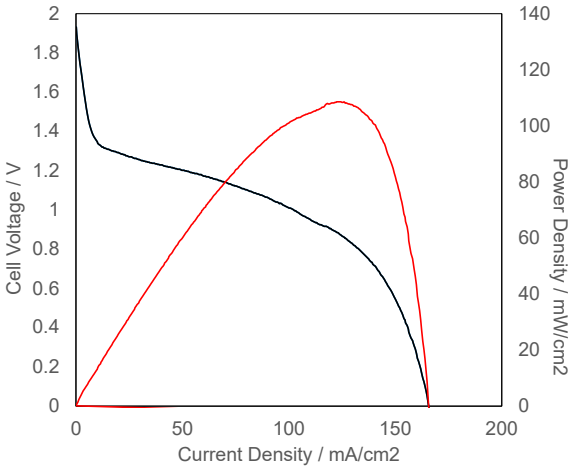

Figure S10. I-V and I-P polarization curves of the paper battery cell with using Pt/C as a cathode electrocatalyst.

S15. Demonstration of paper battery cell performance with bending

See video image, S15.